ELSEVIER

Biochimica et Biophysica Acta 1512 (2001) 345–356

BIOCHIMICA ET BIOPHYSICA ACTA
BBA

www.bba-direct.com

Effect of cholesterol on miscibility and phase behavior in binary mixtures with synthetic ceramide 2 and octadecanoic acid. Infrared studies

Hui-Chen Chen [a], Richard Mendelsohn [a,*], Mark E. Rerek [b], David J. Moore [c]

[a] *Rutgers University, Department of Chemistry, Warren Street, Newark, NJ 07102, USA*
[b] *International Specialty Products, Alps Road, Wayne, NJ 07470, USA*
[c] *Unilever Research US, River Road, Edgewater, NJ 07020, USA*

Received 25 January 2001; received in revised form 9 April 2001; accepted 9 April 2001

Abstract

The three main lipid components of the stratum corneum, namely ceramides, free fatty acids and cholesterol, play a fundamental role in the maintenance of the skin barrier. The current investigation is aimed toward understanding the miscibility and intermolecular interactions of these lipids. Toward this end, Fourier transform infrared spectroscopic studies of the three possible equimolar binary mixtures of cholesterol, a synthetic non-hydroxylated fatty acid *N*-acyl sphingosine with a C18 chain length (*N*-stearoylsphingosine, approximating human ceramide 2), and stearic acid were undertaken. The thermotropic responses of the methylene stretching and scissoring vibrations were used to evaluate chain conformation and packing respectively. Selective perdeuteration, of either the stearic acid or the ceramide acid chains, permitted separate and simultaneous evaluation of the conformational order and packing properties of the sphingosine chain, the amide linked fatty acid chains and/or the stearic acid chain. Whereas cholesterol mixed well with ceramide at physiological temperatures, the stearic acid was miscible with the cholesterol only at relatively high temperatures where the fatty acid is disordered. A complex interaction between stearic acid and ceramide was detected. A separate fatty acid-rich phase persisted until at least 50°C, whereas at higher temperatures the components appear to be quite miscible. However, a preferential association of the fatty acid with the ceramide base chain is indicated. None of the binary systems studied exhibit miscibility and interactions resembling those in the ternary mixtures of these substances, which is widely used to model stratum corneum. The role of cholesterol in controlling the miscibility characteristics in the ternary system is evident.

Keywords: Ceramide; Stratum corneum; Lipid barrier; Domain

1. Introduction

The outermost layer of the epidermis, the stratum corneum (SC), is responsible for skin permeability, and functions to maintain hydration of the internal components and to offer protection against external insults [1]. The SC is a heterogeneous structure composed of keratin enriched corneocytes embedded in a lamellar lipid matrix [2]. It has been proposed that intercellular lipids play a fundamental role in the function and maintenance of the skin barrier [3]. SC lipids consist mainly of ceramides, free fatty acids, and cholesterol in approximately equimolar concentration [4]. At least seven ceramide classes

* Corresponding author. Fax: +1-973-353-1264;
E-mail: mendelso@andromeda.rutgers.edu

0005-2736/01/$ – see front matter
PII: S0005-2736(01)00339-X

have been isolated; clarification of the precise molecular composition of SC lipids continues to be refined with improved isolation and separation techniques [5–7]. The structure and function of the SC lipid barrier has been probed with a variety of physical techniques such as X-ray diffraction [8,9], differential scanning calorimetry [10,11], electron microscopy [12], nuclear magnetic resonance [13,14], infrared (IR) spectroscopy [11,15,16], and Raman spectroscopy [17,18]. A number of model studies have focused on individual ceramides or equimolar mixtures of a ceramide with a fatty acid and cholesterol. However, only a few studies of hydrated binary SC lipid mixtures have been reported [17,19,20].

The current studies of binary skin lipid mixtures have been undertaken to enhance our understanding of the phase behavior and molecular organization of SC lipids, which in turn will help elucidate the relationship between barrier lipid organization and SC function. The use of binary mixtures provides insight into the role of cholesterol. It is difficult to directly monitor the role of cholesterol by infrared spectroscopy due to a lack of characteristic absorptions with sensitivity to intramolecular and intermolecular interactions. In biophysical studies, the effect of cholesterol is most often seen through its impact on other components, such as the broadening and modulation of phase transitions in phospholipid membranes [21,22]. These effects are evident in ceramide/fatty acid/cholesterol SC lipid systems [23]. In binary systems, the role of cholesterol on each component can be more clearly inferred.

In this study, mixtures of cholesterol (Chol) with either *N*-stearoylsphingosine or stearic acid (SA) were prepared. In addition, the use of deuterated derivatives of either Cer2 or SA in each system permitted the separate and simultaneous evaluation of the conformational order and packing properties of the sphingosine base chains, the amide linked fatty acid chains, and/or the stearic acid chain.

2. Materials and methods

Synthetic non-hydroxylated fatty acid ceramides (*N*-acyl-D-*erythro*-sphingosine) comprising amide linked fatty acid chains of stearic acid (Cer2) were purchased from Northern Lipids (Vancouver, Canada). An equivalent ceramide with perdeuterated fatty acid chains (Cer2-d_{35}) was also purchased from the same source. Deuterated stearic acid (SA-d_{35}) was obtained from CDN Isotopes (Quebec, Canada). Proteated stearic acid (SA or SA-h_{35}) and cholesterol (Chol) were purchased from Sigma Chemical Co. (St. Louis, MO). All materials were used without further purification. The chemical structure of Cer2 is shown in Fig. 1.

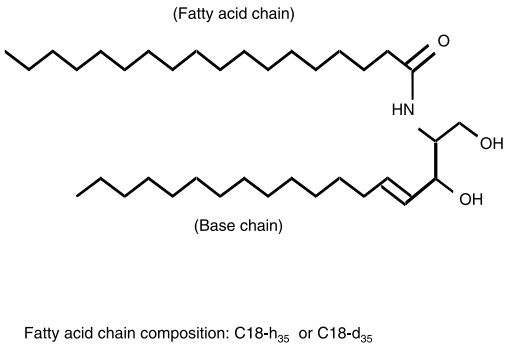

Fig. 1. The chemical structure of *N*-stearoylsphingosine.

Binary lipid systems were prepared by dissolving Cer2/SA, SA/Chol, and Cer2/Chol (1:1 molar ratios in all cases) in chloroform/methanol (2:1, v/v). Appropriate amounts of sample solution were spread and dried onto a ZnSe ATR crystal mounted in a trough plate and placed in a temperature-controlled, horizontal ATR device (Spectra-Tech, Shelton, CT). The dried lipid films were hydrated by covering with excess H_2O or D_2O buffers containing 150 mM NaCl, 4 mM EGTA, and 100 mM citrate, at pH 5.5 (generally considered to be the pH of the SC). A cover plate was placed over the trough to prevent buffer evaporation. Spectra were acquired on a Mattson RS1 spectrometer equipped with a broad band mercury–cadmium telluride (MCT) detector and kept under continuous dry air purge. Spectra were generated by co-addition of 256 interferograms collected at 2 cm^{-1} resolution, and routinely acquired at 2°C intervals from 25°C to 90°C. Samples were allowed to equilibrate for 4–5 min between each temperature increment. Each experiment required approximately 3 h to complete. Equilibration times were varied between duplicate runs and no significant differences in sample thermotropic responses were observed. IR spectra were analyzed off-line using software written at the National Research Council of Canada. Figures

were generated using Sigma Plot 5.0 (SPSS, Chicago, IL).

3. Results

3.1. Cer2-d_{35} and Cer-d_{35}/Chol

The phase transition, conformational order, and packing arrangement of the Cer2 fatty acid and base chains are monitored individually in the presence of Chol as shown in Fig. 2. As controls, frequency versus temperature plots from the thermotropic behavior of the methylene (CH_2 or CD_2) stretching or scissoring vibrations for the Cer2 base chain ($\nu_{sym}CH_2$, δCH_2) and for the Cer2 acid chain ($\nu_{sym}CD_2$, δCD_2) are plotted in Fig. 2A,E,B,F, respectively. The plot of $\nu_{sym}CH_2$ for the base chain of Cer2 (Fig. 2A) shows clear evidence of a solid–solid transition centered at ~70°C and characterized by an increase in frequency from 2848.5 to 2850 cm^{-1}. This is followed by the main order–disorder transition at ~92°C. However, as monitored via the thermotropic response of $\nu_{sym}CD_2$ in Fig. 2B,

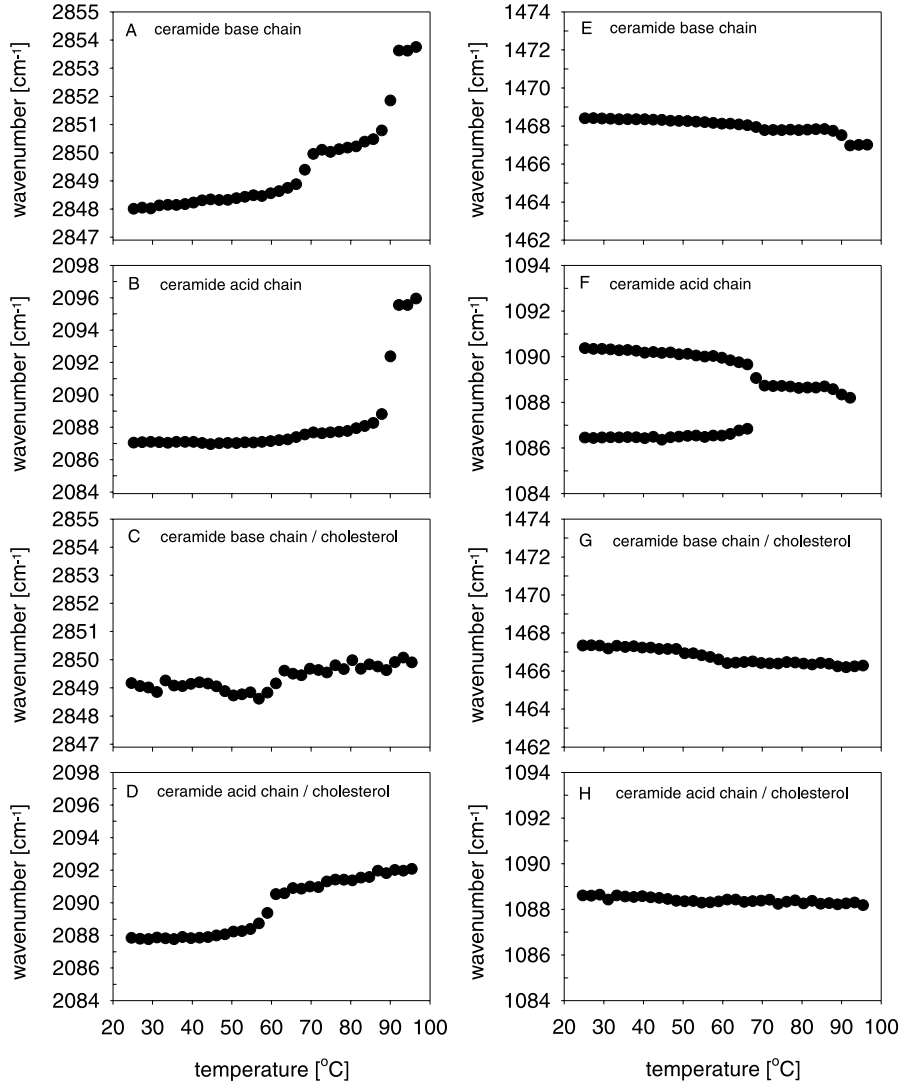

Fig. 2. (A–D) Thermotropic response of $\nu_s CH_2$ from the ceramide base chain, and $\nu_s CD_2$ and from the ceramide acid chain of a pure hydrated Cer2-d_{35} sample (A and B, respectively) and from a hydrated Cer2-d_{35}/Chol (1:1) sample (C and D, respectively). (E–H) Thermotropic response of δCH_2 from the ceramide base chain, and δCD_2 and from the ceramide acid chain of pure a hydrated Cer2-d_{35} sample (E and F, respectively) and from a hydrated Cer2-d_{35}/Chol (1:1) sample (G and H, respectively).

the Cer2 acid chain does not show a significant solid–solid transition before its major melting transition at 92°C. The packing properties of the Cer2 base and acid chains are monitored via the δCH_2 and δCD_2 modes as plotted in Fig. 2E,F, respectively. The δCH_2 mode of the ceramide base chain (Fig. 2E) shows a single component at almost constant frequency (1468.5 cm^{-1}) through all temperatures, although there is a slight decrease in frequency at $\sim$68°C (to 1468 cm^{-1}) and a $\sim$1 cm^{-1} drop at the main chain melt. However, the δCD_2 mode of the ceramide fatty acid chain reveals a clear splitting at 1086.5 and 1090.5 cm^{-1} initially (Fig. 2F) which collapses to a single peak (1088 cm^{-1}) at $\sim$67°C.

The Cer2/Chol binary mixture demonstrates significantly different thermotropic behavior than Cer2 alone. The $\nu_{sym}CH_2$ frequency from the ceramide base chain undergoes a small increase from 2849 to 2850 cm^{-1} at $\sim$60°C (Fig. 2C) which likely represents a loosening of chain packing rather than conformational disordering of the base chain. At the same temperature, the CD_2 stretching mode frequency of the ceramide acid chain increases from 2088 $\rightarrow$ 2090.5 cm^{-1} (Fig. 2D). In neither case is a main order $\rightarrow$ disorder transition observed. Furthermore, both δCH_2 and δCD_2 of the ceramide base chain and ceramide acid chains (Fig. 2G,H, respectively) exhibit single peaks at all temperatures, although a 1 cm^{-1} decrease in δCH_2 is observed at 60°C. Despite the small changes in the methylene stretching modes observed near 60°C for both the ceramide base and acid chains, the data show that at all temperatures both chains are conformationally ordered in the presence of cholesterol.

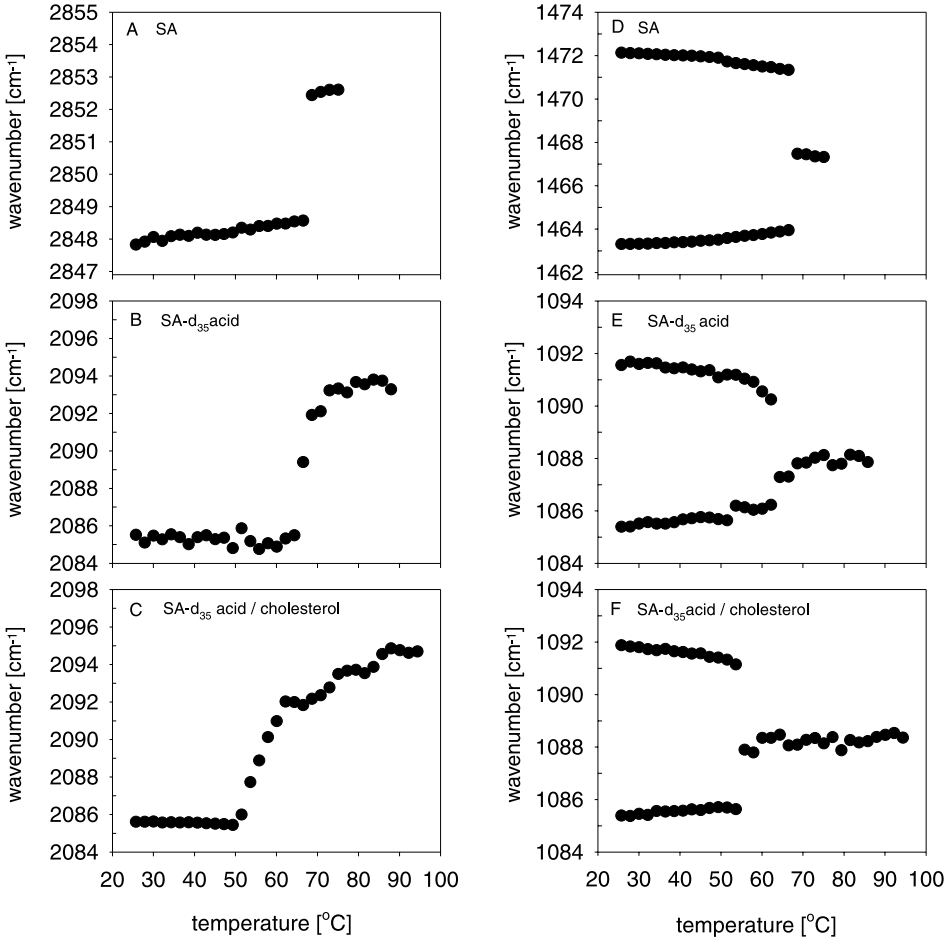

Fig. 3. The thermotropic responses of $\nu_s CH_2$ and δCH_2 from pure stearic acid (SA) are shown in A and D, respectively, while those of $\nu_s CD_2$ and δCD_2 from pure deuterated stearic acid (SA-d_{35}) are shown in B and E, respectively. The thermotropic responses of $\nu_s CD_2$ and δCD_2 from SA-d_{35} in a hydrated SA-d_{35}/Chol mixture are shown in C and E, respectively.

3.2. SA and SA-d_{35} acid/Chol

Plots of the thermotropic behavior of $\nu_{sym}CH_2$ and δCH_2 for pure SA-h_{35} are shown in Fig. 3A,D, respectively. The $\nu_{sym}CH_2$ plot reveals (Fig. 3A) a main order (solid)→disorder (liquid) transition at ~67°C accompanied by a frequency increase from 2848.7 to 2852.5 cm^{-1}. In addition, at ~65°C, the δCH_2 scissoring band splittings (1463, 1472 cm^{-1}) collapse (Fig. 3D) to a single peak at ~1467.5 cm^{-1}. Plots of frequency versus temperature for $\nu_{sym}CD_2$ and δCD_2 modes of pure SA-d_{35} are shown in Fig. 3B,E, respectively. The $\nu_{sym}CD_2$ plot reveals (Fig. 3B) the main order (solid)→disorder (liquid) transition at ~65°C accompanied by a frequency increase from ~2085 to ~2094 cm^{-1}. At ~62°C, the δCD_2 scissoring band splitting (1085.4, 1091.7 cm^{-1} at low temperatures) collapses (Fig. 3E) to a single peak at ~1088 cm^{-1}.

The SA-d_{35}/Chol melting profiles are presented Fig. 3C,F. Two effects on the melting behavior of SA-d_{35} are seen. The first is a broadening of the transition to a width of ~10°C, compared to the pure fatty acid where the width is ~2–4°C. Second, the midpoint is shifted down to ~55°C from ~65°C. Furthermore, the δCD_2 splitting, clearly evident at low temperatures at 1085 and 1091.9 cm^{-1},

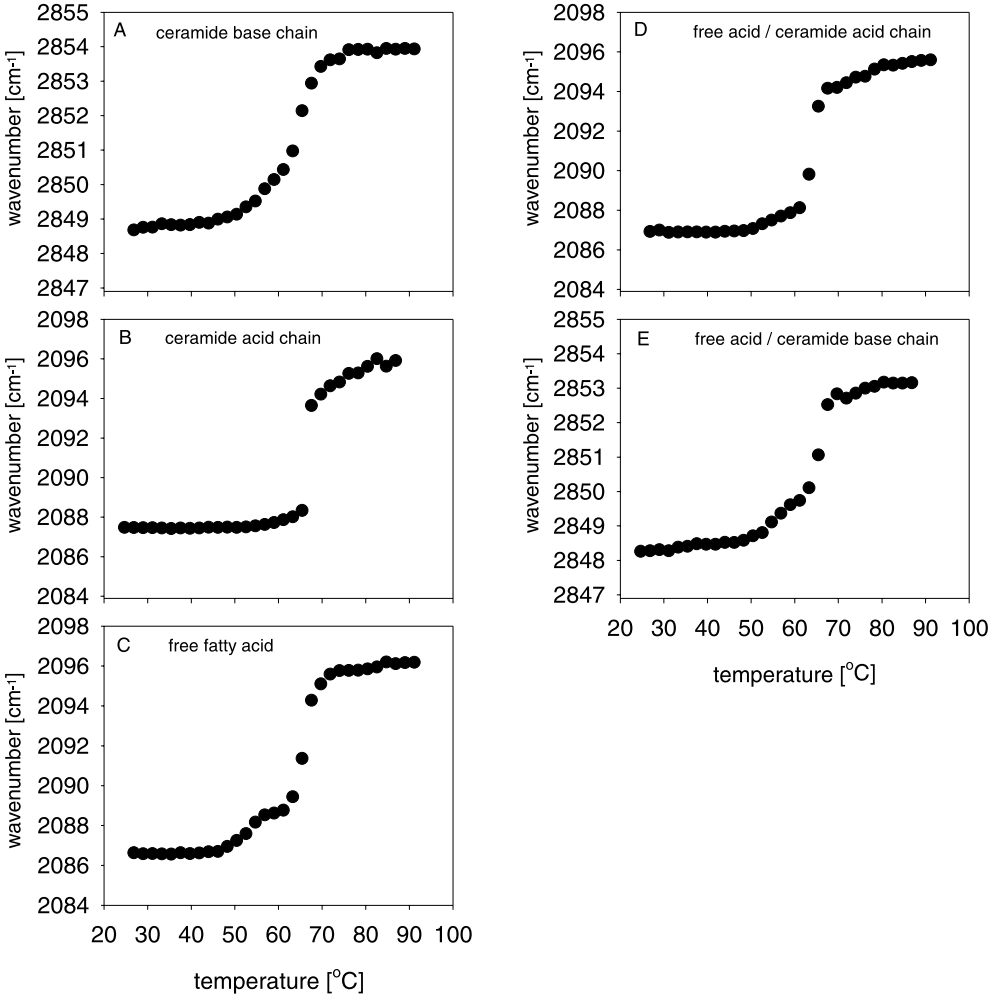

Fig. 4. The thermotropic response of ν_sCH_2 from the ceramide base chain (in a Cer-d_{35}/SA-d_{35} mixture), ν_sCD_2 from the ceramide acid chain (in a Cer-d_{35}/SA mixture), and ν_sCD_2 of SA-d_{35} (in a Cer-h_{35}/SA-d_{35} mixture) are shown in A, B and C, respectively. (D) Thermotropic response of the averaged ν_sCD_2 from the ceramide acid and stearic acid chains in a Cer-d_{35}/SA-d_{35} mixture. (E) Thermotropic response of the averaged ν_sCH_2 from the ceramide base and stearic acid chains in a Cer-d_{35}/SA mixture.

collapses at 55°C to a single peak at 1088 cm^{-1} (Fig. 3F).

3.3. Binary SC lipid mixtures of Cer2-h_{35}/SA-d_{35}, Cer2-d_{35}/SA-d_{35}, and Cer2-d_{35}/SA

Perdeuteration of the Cer2 stearic acid chain or the stearic acid in the above binary mixtures permits the phase behavior and organization of the Cer2 fatty acid chain, base chain, or stearic acid chain to be specifically and directly monitored. In Fig. 4A, the thermotropic response of the $\nu_{sym}CH_2$ from the Cer2 base chain is plotted, and reveals at least two overlapped melting processes (melting range 50–70°C) characterized by an overall frequency increase from ~2848.7 to 2854 cm^{-1}. Fig. 4B shows the $\nu_{sym}CD_2$ frequency from the perdeuterated Cer2 acid chain undergoing a cooperative phase transition from a highly ordered phase (2087.5 cm^{-1}) to a disordered phase (2094 cm^{-1}) with a T_m of ~67°C. The $\nu_{sym}CD_2$ data from SA-d_{35} clearly reveals two transitions as indicated in Fig. 4C. The first, characterized by a frequency increase of ~2 cm^{-1} (from a low-frequency value of ~2087 cm^{-1}) occurs with a midpoint of approximately 53°C. As the temperature is increased, a second highly cooperative transition is observed, characterized by a frequency increase from 2089 → 2096 cm^{-1} centered at 66°C.

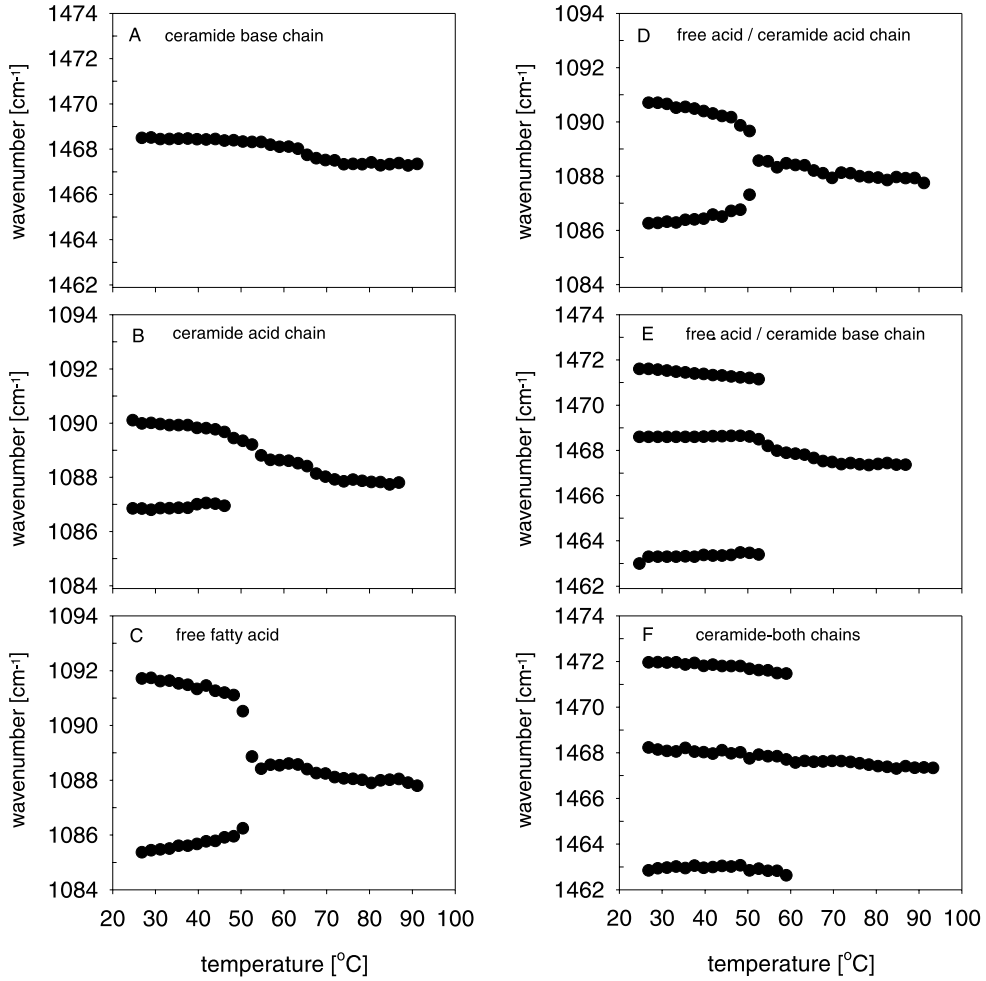

Fig. 5. The thermotropic response of δCH_2 from the ceramide base chain (in a Cer-d_{35}/SA-d_{35} mixture), δCD_2 from the ceramide acid chain (in a Cer-d_{35}/SA mixture), and δCD_2 of SA-d_{35} (in a Cer-h_{35}/SA-d_{35} mixture) are shown in A, B and C, respectively. (D) Thermotropic response of the averaged δCD_2 from the ceramide acid and stearic acid chains in a Cer-d_{35}/SA-d_{35} mixture. (E) Thermotropic response of the averaged δCH_2 from the ceramide base and stearic acid chains in a Cer-d_{35}/SA mixture. (F) Thermotropic response of the averaged δCH_2 from both of the ceramide chains in a Cer-h_{35}/SA-d_{35} mixture.

Fig. 4D displays the melting behavior for $\nu_{sym}CD_2$, which reflects the average behavior of the stearic acid and Cer2 acid chains in the Cer2-d_{35}/SA-d_{35} mixture (only the cer2 base chain is proteated). The initial frequency is low (2087 cm^{-1}) indicating that the chains are tightly packed and in the fully extended all-*trans* conformation. An increase in rotational freedom, due to loosening of chain packing, is observed between 50 and 62°C as manifest by a 1 cm^{-1} change in frequency from 2087 and 2088 cm^{-1}. This is followed by a further cooperative 6 cm^{-1} increase centered at ~66°C. A plot of the averaged $\nu_{sym}CH_2$ frequency from the SA and Cer2 base chains as a function of temperature, is displayed in Fig. 4E. The low and relatively constant value of $\nu_{sym}CH_2$ (2848.3 cm^{-1}) indicates that these chains are highly ordered from 20–50°C. The introduction of conformational disorder and rotational freedom (i.e., loosening of chain packing) begins at 52°C with a frequency increase of ~1 cm^{-1}. The system undergoes a second phase transition from 62°C to 67°C, characterized by an increase in $\nu_{sym}CH_2$ to 2853 cm^{-1}. It is interesting to note that while each chain in Fig. 4 is spectroscopically isolated, in all cases the main transition for the isolated chain is centered at ~66°C.

The temperature induced variation in the δCH_2 of the Cer2 base chain is plotted in Fig. 5A. An initial single peak is seen at ~1468.5 cm^{-1}, which then decreases slightly at 64°C to 1467.5 cm^{-1}. However, the components of the CD_2 scissoring modes from the perdeuterated acyl acid chains of Cer2 exhibit different behavior (Fig. 5B). At temperatures <47°C, the mode is split with components near 1086.9 and 1090.1 cm^{-1} then collapses to a single peak at 1089 cm^{-1}, and undergoes a further overall decrease in frequency of ~1 cm^{-1} between 60°C and 75°C. The splitting is indicative of chains packed in an orthorhombic perpendicular subcell. In Fig. 5C, the δCD_2 bands of SA-d_{35} in the binary mixture show an initial splitting with bands at 1085.3 and 1091.8 cm^{-1}. This is followed by a monotonic decrease in the magnitude of the splitting such that the peaks are at ~1086.3 and 1090.5 cm^{-1} at 50°C. The splitting collapses to a single peak (1088 cm^{-1}) at 54°C. The δCD_2 modes averaged from the SA-d_{35} and Cer2 acid chains are also split as shown in Fig. 5D. At lower temperatures the mode is split into components of 1086.2 and 1090.8 cm^{-1} followed by a collapse at 52°C to 1088.5 cm^{-1}, with further minor decreases at higher temperatures.

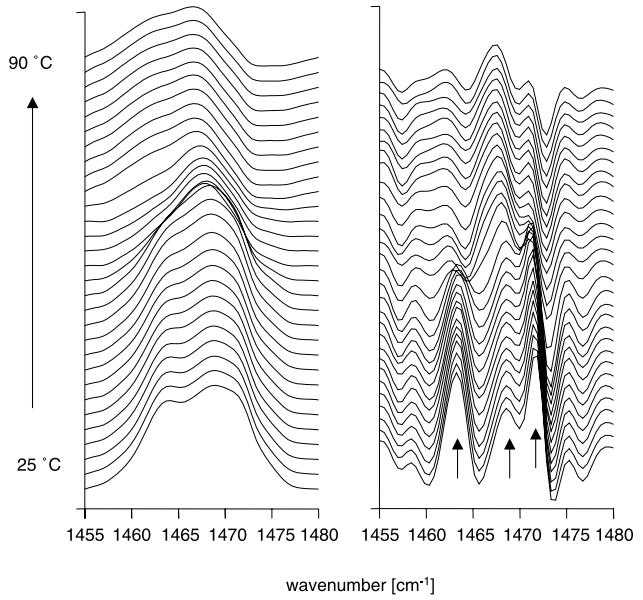

Fig. 6. (A) Original spectra showing the δCH_2 spectral region in a Cer-d_{35}/SA mixture from 25 to 90°C. (B) Inverted second-derivative spectra clearly show the presence of three major bands at temperatures below ~53°C.

Three peaks are clearly noted in the second derivative plots of the Cer2-d_{35}/SA mixture. Original and inverted second derivative spectra for the scissoring region of a Cer2-d_{35}/SA mixture are shown in Fig. 6A,B, respectively. The splitting of δCH_2 modes from the SA-h_{35} and Cer2 base chain are plotted in Fig. 5E. The CH_2 bending modes at 25–54°C indicate a clear presence of two components at 1463.1 and 1471.7 cm^{-1} which collapse into one band at 53°C. In addition, a band appears at low temperatures at 1468.6 cm^{-1} and exhibits a monotonic decrease in frequency beginning at 55°C. Similar effects are noted (Fig. 5F) for the sample in which both Cer2 chains are proteated, although the temperature at which the splitting collapses is increased to ~59°C.

3.4. Ternary SC lipid mixture of Cer2-h_{35}/SA-h_{35}/Chol

In Fig. 7, the average thermotropic effect on both

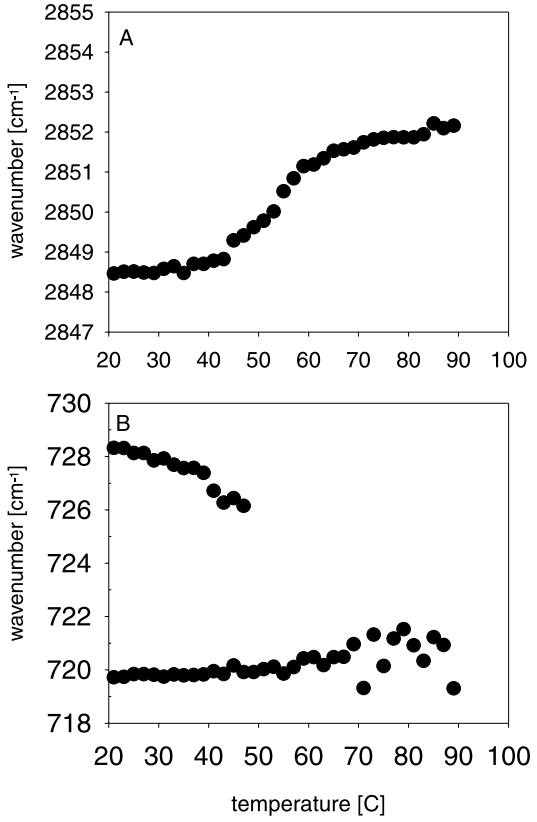

Fig. 7. (A) Thermotropic response of $\nu_s CH_2$ averaged from all components in a ternary mixture of Cer-h_{35}/SA/Chol. (B) Thermotropic response of δCH_2 averaged from all components in a ternary mixture of Cer-h_{35}/SA/Chol.

$\nu_{sym}CH_2$ and δCH_2 for both Cer2 and SA is shown. Fig. 7A gives the average $\nu_{sym}CH_2$ for the ternary mixture. The system is very ordered at room temperature with $\nu_{sym}CH_2$ at 2848.5 cm^{-1}. A broad disordering/packing alteration between 45 and 55°C is manifest as a change in frequency from 2848.5 to 2850 cm^{-1}. This is followed by a broad transition from 55°C to 65°C with a change in frequency from 2850 to 2852 cm^{-1}. Full disordering is not observed as the average $\nu_{sym}CH_2$ remains near 2852 cm^{-1}.

Chain packing can be determined through the CH_2 rocking mode (Fig. 7B). At temperatures <40°C, the mode is split with components near 728 and 720 cm^{-1}. The splitting is indicative of chains packed in an orthorhombic perpendicular subcell, which collapses to a single peak at 720 cm^{-1} at 47°C and undergoes a further increase in frequency of ~ 1 cm^{-1} between 65°C and 75°C.

4. Discussion

To elucidate the unique nature of SC, and to enhance current understanding of the phase behavior and molecular organization of SC lipids, we have undertaken studies of binary mixtures of skin lipids. Previous experiments focused on fatty acid chain homogeneous Cer2 in which the acid chains (lengths C14, C16, C18 and C20) were perdeuterated [24]. As noted in the introduction, the use of binary mixtures provides further insights into the role of cholesterol. In the current report the miscibility of cholesterol with either Cer2 or with SA is explored via the thermotropic behavior of methylene vibrations sensitive to both intermolecular and intramolecular chain behavior. Utilizing isotopically labeled SA and Cer2 in mixtures with Chol minimizes the potential interference from Chol vibrations. This approach permits some detailed structural conclusions to be reached.

At an equimolar ratio, Chol and Cer2 are well mixed at physiological temperatures. Comparing Fig. 2A with C and Fig. 2B with D indicate that an equimolar amount of Chol abolishes the main order–disorder transition of both the Cer2 base and acid chains. The small increase in $\nu_{sym}CH_2$ at ~ 60°C probably reflects a loosening of chain packing rather than significant fluidizing of the Cer2 base chains since $\nu_{sym}CH_2$ remains below 2850 cm^{-1} at all temperatures. Similarly, the 2 cm^{-1} increase in $\nu_{sym}CD_2$ may result from an increased rotational freedom of the Cer2 acid chains, rather than significant conformational disordering. The miscibility of Chol with Cer2 is also suggested from the absence of splitting of the CD_2 scissoring band in the Cer2 acid chain (Fig. 2H), compared with pure Cer2.

In contrast to Cer2, there is a lack of miscibility of SA in its ordered phase with Chol at an equimolar ratio as shown in Fig. 3F. The scissoring vibrations of the SA-d_{35} reveal maximal (~ 7 cm^{-1}) splitting. Thus the presence of Chol does not disrupt the crystalline SA domains at low temperature. In contrast, Chol broadens the main order→disorder transition of SA so that the disordering occurs over a 10°C range compared with 1°C range for the pure fatty acid (Fig. 3C). In addition the midpoint is shifted lower by ~ 9°C compared with pure SA-d_{35}. These observations point to a miscibility of the fatty acid

with the cholesterol only at high temperatures where the fatty acid is disordered. The overall behavior is consistent with a eutectic-melting phenomenon.

The proteated base (Fig. 4A) chain and deuterated acid chain (Fig. 4B) of Cer2 in the appropriate binary mixture with SA exhibit different melting profiles. Although both chains show evidence of transitions involving the introduction of substantial conformational disorder, the increase in base chain fluidity occurs over an 8°C range (62–70°C), while the acid chain disorders abruptly at 67°C. Furthermore, the base chain undergoes an additional, less cooperative chain disordering process from 52°C to 62°C as indicated by $\nu_{sym}CH_2$ increasing from $\sim$2849 to $\sim$2850.9 cm^{-1}. These data suggest that the ceramide acid chains are more tightly packed (and thus exhibit more highly cooperative melting) than the base chains, even in the presence of fatty acid.

The miscibility of the components in Cer2/SA mixtures is deduced by comparing the melting profiles of each chain in the mixture with those of the pure components. The following transition temperatures were observed for the main order–disorder event: fatty acid homogeneous Cer2, $\sim$92°C (see Fig. 2A,B); SA-h_{35}, 68–69°C; SA-d_{35} (65–66°C). In binary mixtures, the main SA melting is only slightly perturbed (Fig. 4C) from the pure component (Fig. 3B). The low temperature transition noted for this component of the binary mixture probably reflects formation of hexagonally packed chains (loss of orthorhombically packed perpendicular packing) from 47°C to 55°C, prior to the main chain melt (Fig. 5C). For pure SA-d_{35}, the scissoring splitting collapse temperature coincides with the main order–disorder transition. The high temperature melting transition profile for SA-d_{35} accurately parallels that of the Cer2 base chains. The main chain melting of Cer2 in the binary mixture is 30°C lower than in the pure component. Taken together, these observations suggest that, at high temperatures, the two components are miscible, and that preferential association of the fatty acid occurs with the base chain.

The microdomain structure and miscibility of the low temperature phases in the Cer2/SA mixture may be deduced from the methylene scissoring mode contours. As analyzed in detail by Snyder and his coworkers, the scissoring contour splits into a doublet for methylene chains packed in an orthorhombic perpendicular arrangement [25–27]. The maximal splittings for C18 chains are $\sim$1462, 1473 cm^{-1} for proteated chains and $\sim$1085, 1092 cm^{-1} for deuterated chains. The splitting arises from short-range vibrational coupling between isotopically alike, adjacent chains. Thus, the presence of small domains of a particular isotopically labeled molecule may be directly inferred from the presence of two components of the scissoring contour. Recent reviews by Mendelsohn and Moore have discussed the use of this parameter in biophysical spectroscopy [28,29].

The occurrence of large domains of SA-d_{35} in the ordered phase of the mixture is evident from observations of the full splitting of the scissoring doublet (Compare Fig. 5C with Fig. 3E). This provides direct evidence for the existence of a separate fatty acid-rich phase which persists at least until the collapse of the splitting at $\sim$50°C. Examination of the CD_2 scissoring contour of the original or second derivative spectra at temperatures below the collapse suggests that most of the SA-d_{35} is phase separated. If a significant proportion of this component were mixed with Cer2, then a peak arising from CD_2 scissoring modes in isolated chains would have been observed at $\sim$1089 cm^{-1} at temperatures $< \sim$50°C. This was not the case.

The behavior of the scissoring modes of the Cer2 component is quite different from the fatty acid. The isolated, proteated base chain, although ordered (as deduced from the $\nu_{sym}CH_2$) exhibits no splitting (Fig. 5A), while the isolated acid chain (Fig. 5B) exhibits slight splitting. An estimate of the acid chain domain size of the Cer2 acid chain from the published calibration curve suggests the presence of $\sim$3–5 chains/domain [27]. Since the low temperature data for Cer2 in the mixture are very similar to those of pure Cer2, the results for this component, as for the SA, again indicate that the ordered phases of Cer2 and SA do not mix substantially. The scissoring splitting in the acid chains is reduced from the maximum value because of the small domain size and the presence of proteated base chains. The absence of splitting of the base chain scissoring modes indicates these chains are not packed in orthorhombic perpendicular domains, and/or that they are geometrically packed in a way that eliminates vibrational interactions between them. The δCH_2 data from the binary mixture in which only the Cer2 acid chain is deuterated are

plotted in Fig. 5E. Comparison of Fig. 5A with C provides an assignment for these branches. The high- and low-frequency branches at temperatures below ~55°C are assigned to the SA, while the central branch arises from the scissoring modes of the ceramide base chain.

The δCH_2 spectra from the binary mixture in which the SA is deuterated are shown in Fig. 6 and the temperature dependence of the scissoring mode branches is plotted in Fig. 5F. Comparison with Fig. 5A,B provides an assignment for these branches. The high and low frequency branches at temperatures below ~55°C are assigned to the acid chain. The splitting is enhanced as compared to Fig. 5B for two reasons. First, the magnitude of the splitting in proteated chains is $\sqrt{2}$ times greater than deuterated domains of the same size. In addition, there are further interactions between some acid and base chains that enhance the splitting. Nevertheless, the presence of some vibrationally uncoupled chains is still clear, from the observation of the central branch in Fig. 5F.

The average CH_2 stretching and rocking modes for the ternary combination of fully proteated, equimolar Cer2/SA/Chol are shown in Fig. 7A,B, respectively. The use of fully proteated molecules gives an average over all three components for both the chain order (CH_2 stretching) and chain packing (CH_2 rocking). The breadth of the transition and the failure to reach full chain disordering are signatures of mixing with cholesterol during this transition. The fact that only one transition is observed is also consistent with both Cer2 and SA undergoing the disordering process in concert. From 30°C to 40°C there is a reduction in the splitting of the CH_2 rocking mode from 8 to 6 cm^{-1}, indicating the orthorhombic domains are getting smaller. Band splitting collapses at about 45°C, as $\nu_{sym}CH_2$ increases from 2849 to 2850 cm^{-1}.

5. Concluding remarks

We have previously evaluated chain order and phase behavior of ternary lipid models in which ceramide 2 is fully proteated and the fatty acid is deuterated [24]. These systems always show separate orthorhombic domains of ceramide and fatty acid (indicated by splitting in both the δCH_2 and δCD_2 modes) that undergo broad phase transitions at temperatures significantly reduced from the pure components. The binary skin lipid systems described here all display thermotropic phase behaviors that are distinct from the ternary lipid system most used to model the stratum corneum. It is concluded that these differences provide a significant rationale for all three lipid species being required for a healthy stratum corneum barrier. We speculate that, since cholesterol loosens the chain packing of the ceramide in binary mixtures, if only ceramides and cholesterol were present in vivo, the barrier would be much more permeable and might not contribute the proper environment for exogenous enzymes to function. A lipid barrier comprised of only ceramides and fatty acids would be too rigid under physiological conditions and would likely not display satisfactory mechanical properties for the skin. Although the fatty acid and cholesterol system most resembles the ternary lipid system at room temperature, the extensive mixing upon fluidization might not sufficiently resist environmental stress or properly demix upon synthesis from their precursors in the extracellular matrix.

Biophysical studies of the main components of the barrier permit a molecular level understanding of their structures and interactions. The use of perdeuterated lipid chains permits the IR spectroscopic evaluation of individual chain structure and mixing behavior. The current approach, in conjunction with earlier studies of ternary models [15,23,20] and studies of polar region structures [30,31] and interactions, paves the way for the extension of the IR approach to skin biophysics. This includes studies of reconstituted systems such as lipid-free corneocytes reinserted into lipid environments and exogenous lipids added either to model stratum corneum or to skin itself. In addition, determination of the effects of exogenous compounds on the structure and interaction of the skin barrier constituents is clearly feasible.

In a more general way, the strategies for characterization of domains by IR spectroscopy as presented here may be useful in studies of lipid distributions in sphingolipid and cholesterol-based structures Recently (see [32] for a review), much attention has been focused on detergent-resistant membrane fragments that can be isolated from a variety of mammalian cells. The presence of relatively ordered, well-packed phases seems to be important for the forma-

tion of these so-called membrane rafts. If chain perdeuterated sphingolipids become available, and suitable protocols for their insertion into membranes are developed, then chain–chain interactions between deuterated chains may be sought for in the IR spectral parameters of the labeled moieties. The feasibility of this approach has been demonstrated from this laboratory for characterization of particular phospholipid classes in red blood cells [33,34].

Acknowledgements

This work was supported in part by US-PHS Grant GM 29864 to R.M.

References

[1] B. Forslind, The skin: upholder of physiological homeostasis. A physiological and (bio)physical program, Thromb. Res. 80 (1995) 1–22.
[2] H. Schaefer, T.E. Redelmeier, Skin Barrier: Principles of Percutaneous Absorption, Karger, Basel, 1996.
[3] P.M. Elias, Epidermal barrier function: intercellular lamellar lipid structures, origin, composition and metabolism, J. Controlled Release 15 (1991) 199–208.
[4] P.W. Wertz, B. van den Bergh, The physical, chemical and functional properties of lipids in the skin and other biological barriers, Chem. Phys. Lipids 91 (1998) 85–96.
[5] P.W. Wertz, M.C. Miethke, S.A. Long, J.S. Strauss, D.T. Downing, The composition of the ceramides from human stratum corneum and from comedones, J. Invest. Dermatol. 84 (1985) 410–412.
[6] K.J. Robson, M.E. Stewart, S. Michelsen, N.D. Lazo, D.T. Downing, 6-Hydroxy-4-sphingenine in human epidermal ceramides, J. Lipid Res. 35 (1994) 2060–2068.
[7] M.E. Stewart, D.T. Downing, A new 6-hydroxy-4-sphingenine-containing ceramide in human skin, J. Lipid Res. 40 (1999) 1434–1439.
[8] T.J. McIntosh, M.E. Stewart, D.T. Downing, X-ray diffraction of isolated skin lipids: reconstitution of intercellular lipid domains, Biochemistry 35 (1996) 3649–3653.
[9] J.A. Bouwstra, J. Thewalt, G.S. Gooris, N. Kitson, A model membrane approach to the epidermal permeability barrier: An X-ray diffraction study, Biochemistry 36 (1997) 7717–7725.
[10] C.-H. Han, R. Sanftleben, T.S. Wiedmann, Phase properties of mixtures of ceramides, Lipids 30 (1995) 121–128.
[11] G.M. Golden, D.B. Guzek, R.R. Harris, J.E. McKie, R.O. Potts, Lipid thermotropic transitions in human stratum corneum, J. Invest. Dermatol. 86 (1986) 222–259.
[12] G. Menon, R. Ghadially, Morphology of lipid alterations in the epidermis: A review, Microsc. Res. Tech. 37 (1997) 180–192.
[13] J. Thewalt, N. Kitson, C. Araujo, A. MacKay, M. Bloom, Models of stratum corneum intercellular membranes: The sphingolipid headgroup is a determinant of phase behavior in mixed lipid dispersions, Biochem. Biophys. Res. Commun. 188 (1992) 1247–1252.
[14] N. Kitson, J. Thewalt, M. Lafleur, M. Bloom, A model membrane approach to the epidermal permeability barrier, Biochemistry 33 (1994) 6707–6715.
[15] D.J. Moore, M.E. Rerek, R. Mendelsohn, Lipid domains and orthorhombic phases in model stratum corneum: Evidence from Fourier transform infrared spectroscopy studies, Biochem. Biophys. Res. Commun. 231 (1997) 797–801.
[16] M. Lafleur, Phase behavior of model stratum corneum lipid mixtures: an infrared spectroscopy investigation, Can. J. Chem. 76 (1998) 1501–1511.
[17] M. Wegener, R. Neubert, W. Rettig, S. Wartewig, Structure of stratum corneum lipids characterized by FT-Raman spectroscopy and DSC. III. Mixtures of ceramides and cholesterol, Chem. Phys. Lipids 88 (1997) 73–82.
[18] R. Neubert, W. Rettig, S. Wartewig, M. Wegener, A. Wienhold, Structure of stratum corneum lipids characterized by FT-Raman spectroscopy and DSC. II. Mixtures of ceramides and saturated fatty acids, Chem. Phys. Lipids 89 (1997) 3–14.
[19] D.T. Parrott, J. E Turner, Mesophase formation by ceramides and cholesterol: a model for stratum corneum lipid packing, Biochim. Biophys. Acta 1147 (1993) 273–276.
[20] C.R. Flach, R. Mendelsohn, M.E. Rerek, D.J. Moore, Biophysical studies of model stratm corneum lipid monolayers by infrared reflection-absorption spectroscopy and Brewster angle microscopy, J. Phys. Chem. 104 (2000) 2159–2165.
[21] O.G. Mouritsen, K. Jorgsesen, Dynamical order and disorder in lipid bilayers, Chem. Phys. Lipids 73 (1994) 3–25.
[22] J. Ipsen, G. Karlstrom, O. Mouritsen, H. Wennerstrom, M. Zuckermann, Phase equilibria in the phosphatidylcholine-cholesterol system, Biochim. Biophys. Acta 905 (1987) 162–172.
[23] D.J. Moore, M.E. Rerek, Insights into the molecular organization of lipids in the skin barrier from infrared spectroscopy studies of stratum corneum lipid models, Acta Derm. Venereol. Suppl. 208 (2000) 16–22.
[24] H. Chen, R. Mendelsohn, M. Rerek, D.J. Moore, Fourier transform infrared spectroscopy and differential scanning calorimetry studies of fatty acid homogeneous ceramide 2, Biochim. Biophys. Acta 1468 (2000) 293–303.
[25] R.G. Snyder, Vibrational spectra of crystalline *n*-paraffins: II. Intermolecular effects, J. Mol. Spec. 7 (1961) 116–144.
[26] R.G. Snyder, Vibrational correlation splitting and chain packing for the crystalline *n*-alkanes, J. Chem. Phys. 71 (1979) 3229–3235.
[27] R.G. Snyder, M.C. Goh, V.J.P. Srivatsavoy, H.L. Strauss, D.L. Dorset, Measurement of the growth kinetics of microdomains in binary *n*-alkane solid solutions by infrared spectroscopy, J. Phys. Chem. 96 (1992) 10008–10019.

[28] R. Mendelsohn, D.J. Moore, Vibrational spectroscopic studies of lipid domains in biomembranes and model systems, Chem. Phys. Lipids 96 (1998) 141–157.
[29] R. Mendelsohn, D.J. Moore, IR determination of conformational order and phase behavior in ceramides and stratum corneum models, in: Y.A. Hannun, A.H. Merrill (Eds.), Methods in Enzymology, Vol. 312, Academic Press, New York, 2000.
[30] D.J. Moore, M.E. Rerek, R. Mendelsohn, FTIR spectroscopy studies of the conformational order and phase behavior of ceramides, J. Phys. Chem. B 101 (1997) 8933–8940.
[31] R. Mendelsohn, M.E. Rerek, D.J. Moore, Infrared spectroscopy and microscopic imaging of stratum corneum models and skin, Phys. Chem. Chem. Phys. 2 (2000) 4651–4657.
[32] D.A. Brown, E. London, Structure and function of sphingolipid-and cholesterol-rich membrane rafts, J. Biol. Chem. 275 (2000) 17221–17224.
[33] D.J. Moore, R.H. Sills, R. Mendelsohn, Conformational order of specific phospholipids in human erythrocytes: Correlations with changes in cell shape, Biochemistry 36 (1997) 660–664.
[34] D.J. Moore, S. Gioioso, R.H. Sills, R. Mendelsohn, Some relationships between membrane phospholipid domains, conformational order, and cell shape in intact human erythrocytes, Biochim. Biophys. Acta 1415 (1999) 342–348.